Tumor Environment Dictates Medulloblastoma Cancer Stem Cell Expression and Invasive Phenotype

Borhane Annabi,[1] Shanti Rojas-Sutterlin,[2] Carl Laflamme,[1] Marie-Paule Lachambre,[2] Yannève Rolland,[2] Hervé Sartelet,[3] and Richard Béliveau[2]

[1]Laboratoire d'Oncologie Moléculaire, Département de Chimie, Université du Québec à Montréal, [2]Centre de Cancérologie Charles-Bruneau, Hôpital Sainte-Justine-UQAM, and [3]Department of Pathology, Hôpital Sainte-Justine, Montreal, Quebec, Canada

Abstract

The neural precursor surface marker CD133 is thought to be enriched in brain cancer stem cells and in radioresistant DAOY medulloblastoma-derived tumor cells. Given that membrane type-1 matrix metalloproteinase (MT1-MMP) expression is a hallmark of highly invasive, radioresistant, and hypoxic brain tumor cells, we sought to determine whether MT1-MMP and other MMPs could regulate the invasive phenotype of CD133(+) DAOY cells. We found that when DAOY medulloblastoma or U87 glioblastoma cells were implanted in nude mice, only those cells specifically implanted in the brain environment generated CD133(+) brain tumors. Vascular endothelial growth factor and basic fibroblast growth factor gene expression increases in correlation with CD133 expression in those tumors. When DAOY cultures were induced to generate *in vitro* neurosphere-like cells, gene expression of CD133, MT1-MMP, MMP-9, and MDR-1 was induced and correlated with an increase in neurosphere invasiveness. Specific small interfering RNA gene silencing of either MT1-MMP or MMP-9 reduced the capacity of the DAOY monolayers to generate neurospheres and concomitantly abrogated their invasive capacity. On the other hand, overexpression of MT1-MMP in DAOY triggered neurosphere-like formation which was further amplified when cells were cultured in neurosphere medium. Collectively, we show that both MT1-MMP and MMP-9 contribute to the invasive phenotype during CD133(+) neurosphere-like formation in medulloblastoma cells. Increases in MMP-9 may contribute to the opening of the blood-brain barrier, whereas increased MT1-MMP would promote brain tumor infiltration. Our study suggests that MMP-9 or MT1-MMP targeting may reduce the formation of brain tumor stem cells. (Mol Cancer Res 2008;6(6):907–16)

Introduction

Recently, a small population of cancer stem cells (CSC) in adult and pediatric brain tumors has been identified (1, 2). These CSC, once isolated from tumor tissues, form neurospheres when cultured *in vitro* and possess the capacity for cell renewal. Based on their high expression of the neural precursor cell surface marker CD133 (prominin-1), these CSC have been further hypothesized to bear properties such as resistance to apoptosis and resistance to drugs and to ionizing radiation (3, 4). Interestingly, among primary human medulloblastoma and glioblastoma multiforme–derived cells, only those cells expressing CD133 on their surfaces can initiate tumors in the brains of nonobese diabetic/severe combined immunodeficient mice (5). In fact, the injection of as few as 100 CD133(+) cells produces a tumor that could be serially transplanted and that is a phenocopy of the patient's original tumor, whereas injection of CD133(−) cells did not cause a tumor. Such evidence highlights the fact that in brain tumors, and in other malignancies, the tumor clone is functionally heterogeneous, existing, however, in a cellular hierarchy based on small subpopulations of stem cells (6).

Given that CD133 has been identified as a powerful CSC marker, and that its gene expression is significantly higher in the recurrent brain tumor tissue, we examined whether other molecular players may also contribute to the invasive potential of medulloblastomas. Matrix metalloproteinases (MMP) have been shown to be associated with glioblastoma (7, 8) and medulloblastoma cell invasiveness (9, 10). In particular, levels of MMP-9 and membrane type-1 (MT1)–MMP expression were increased in >75% of medulloblastoma tumor tissues (11). Whether the CD133(+)-CSC subpopulation of cells was also targeted remains unknown. When *MMP-9* gene expression was silenced in DAOY medulloblastoma-derived cells, experimental *in vivo* tumor growth was inhibited in an intracranial animal model (12). Moreover, in line with the CD133(+) tumor cell phenotype that accounts for glioma stem cells' radioresistance (13), the expression of MT1-MMP expression was also increased in several cell line models that escaped radiation-induced apoptosis (14, 15). Previous reports from our laboratory have documented the contribution of MT1-MMP to the infiltrative and invasive phenotype of brain tumor–derived cells (16, 17), and strategies which inhibit either

MMP-9 or MT1-MMP activities and/or expression may, furthermore, be envisioned to reduce tumorigenicity (17-19). Whether expression of MMP-9 or MT1-MMP affects the acquisition of an invasive phenotype during neurosphere-like formation of CSC is currently unknown.

In this study, we sought to examine the effect of tumor tissue environment and the contribution of CD133(+) brain tumor– derived CSC to tumor development *in vivo*. We also investigated the *in vitro* expression of MMP-9 and MT1-MMP, two MMPs which contribute to the blood-brain barrier opening and to the radioresistance phenotype of brain tumor cells in the neurosphere formation capacity of DAOY medulloblastoma cells.

Results

The Tissue Environment of Cell Implantation Dictates the Expression of CD133(+) Brain Tumor–Derived Stem Cells

In an attempt to assess the contribution of CD133(+) CSC to experimental brain tumor growth, monolayer cultures of DAOY medulloblastoma cells were trypsinized and cell suspensions were implanted either subcutaneously or by stereotaxis within the brain and left to develop for several weeks as described in Materials and Methods. Histopathologic analysis of intracerebrally implanted human DAOY medullo-blastoma cells shows well-defined but not encapsulated large malignant proliferation composed of a majority of small undifferentiated round cells found in normal mouse brain (Fig. 1A1). At high magnification, hematoxylin-phloxin-saffron staining shows that the tumor was highly cellular with numerous mitoses (Fig. 1A2), and presents an aggressive pattern with a limited area of necrosis (Fig. 1A3). The nuclei are often densely hyperchromatic, and are associated with poor cytoplasm. No fibrillar material and no rosette could be identified. Stromal elements were scant, consisting of small blood vessels. Moreover, some tumoral cells were found to exhibit membranous expression of CD133 (Fig. 1A4, *arrows*). Although subcutaneous tumor growth was only observed with implanted U87 glioblastoma cells, we found that U87 and DAOY cells implanted within the cerebral environment readily developed into tumors. Intracerebral growth of U87 tumors was routinely found to occur within the first 2 to 3 weeks, whereas significant intracerebral growth of DAOY tumors only occurred after 9 to 11 weeks. Homogenates were then generated from the individual tumors and CD133 immunodetection was done. We found that CD133 protein expression was only observed when U87 or DAOY cells were implanted within the cerebral environment (Fig. 1B). The origin of CD133 expression was further examined when homogenates from DAOY cell monolayers, control brain hemisphere, and intracerebral DAOY-derived tumors were probed for CD133. We found that DAOY cell monolayers expressed low basal CD133 (Fig. 1C, *in vitro*), whereas CD133 expression was enriched in the brain hemi-sphere in which DAOY cells had been implanted (Fig. 1C, *in vivo*). Quantitative PCR was also done with the control and DAOY-derived tumors and confirmed the angiogenic phenotype of DAOY-derived tumors as vascular endothelial growth factor and basic fibroblast growth factor gene expression were significantly increased in those tumors (Fig. 1D).

Increased CD133, MDR-1, MT1-MMP, and MMP-9 Expression Characterize the Invasive Phenotype of Neurosphere-Like DAOY Cells

Neurosphere-like brain CSC are thought to contribute to a subpopulation of CD133(+) brain CSC (4). Neurosphere induction of DAOY cells was done according to established protocols (20-22), and this process promoted the transition of adherent DAOY monolayer cells to neurosphere-like cells (Fig. 2A). Total RNA was isolated from monolayers and from neurosphere-like DAOY cells and semiquantitative reverse transcription-PCR (RT-PCR) was done. We found that gene expression of CD133, MDR-1, HuR, MMP-9, and MT1-MMP all increased in neurosphere-like DAOY cells (Fig. 2B). Although the increase in CD133 cell surface expression was confirmed in cells cultured in neurospheres by flow cytometry (data not shown), the increases in MMP-9 and in MT1-MMP were both confirmed when conditioned media were isolated from serum-starved monolayers and from neurosphere-like DAOY cells and we observed a massive increase in extracellular proMMP-9 gelatinolytic activity, as assessed by gelatin zymography (Fig. 2C) from the latter medium. Although the latent proMMP-2 extracellular levels remained unchanged between monolayers and neurosphere-like cells, the active forms of MMP-2 were exclusively produced in neurospheres, most likely due to an increased MT1-MMP activity (Fig. 2C). Cell migration was also assessed by seeding monolayers and neurosphere-like DAOY cells on top of modified Boyden chambers. We found that the invasive capacity of neurosphere-like DAOY cells was significantly increased when compared with DAOY cells grown into monolayers (Fig. 2D).

MT1-MMP and MMP-9 Contribute to the Invasive Pheno-type and Contribute to the Neurosphere-Like Formation Process in DAOY Cells

We next assessed the effects of MMP-9 and MT1-MMP activities in promoting neurosphere-like formation and invasion using RNA interference technology. DAOY monolayer cells were transiently transfected with small interfering RNA to specifically down-regulate either MMP-9 or MT1-MMP gene expression as described in Materials and Methods. Transfection efficiencies were monitored either through the protein expres-sion of MMP-9 or through the MT1-MMP–mediated activation of proMMP-2 using gelatin zymography. We found that basal levels of proMMP-9 in DAOY monolayers (Fig. 3A, *monolayers*) as well as the proMMP-9 induced in neurosphere-like DAOY cells (Fig. 3A, *neurospheres*) were significantly decreased in siMMP-9–transfected cells when compared with mock-transfected cells. MT1-MMP was also efficiently silenced and this was reflected by the complete inability of neurosphere-like DAOY cells to activate latent proMMP-2 into its active MMP-2 form (Fig. 3A, *neurospheres*). MT1-MMP pro- and active forms of protein expression are further shown to be efficiently and specifically diminished using immunoblotting in siMT1-MMP–transfected cells but not in siMMP-9–transfected cells (Fig. 3B, *exposition 30 s*). Moreover, the increased proMMP-2 activation observed in neurospheres by zymography (Fig. 3A) also correlates with MT1-MMP proteolytic activation as seen by the appearance of the well-documented 45 kDa MT1-MMP immunoreactive inactive form (Fig. 3B, *exposition 2 min*).
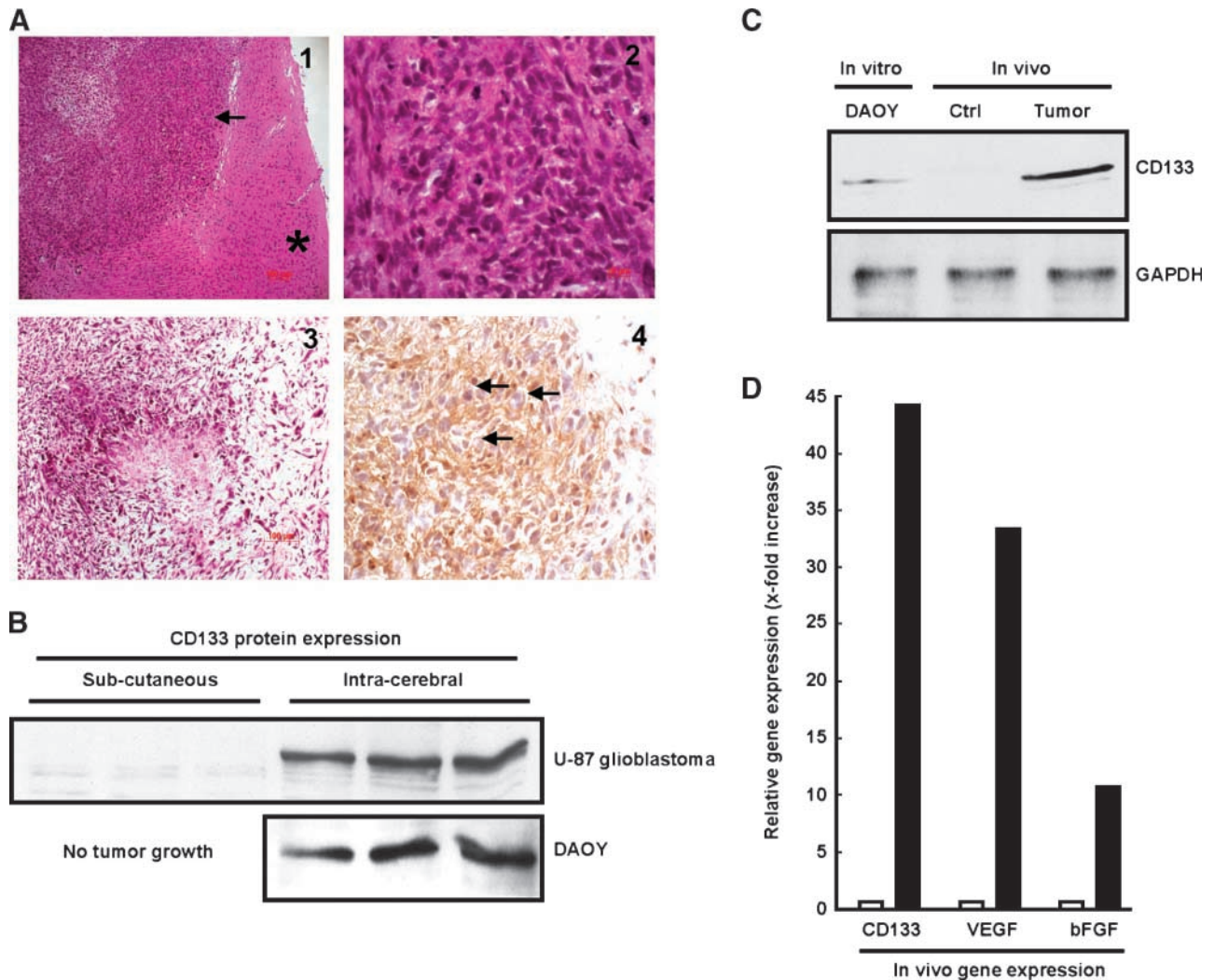
FIGURE 1. The tissue environment of cell implantation dictates the expression of CD133(+) brain tumor–derived stem cells. Cultured DAOY monolayers were trypsinized and 10^6 cells injected either subcutaneously or intracerebrally into nude mice. Tumors were left to develop as described in Materials and Methods. **A.** Histopathologic analysis of paraffin sections (3 μm) of intracerebrally implanted human DAOY medulloblastoma cells was done with hematoxylin-phloxin-saffron staining and shows (*1*) malignant proliferation composed of a majority of small round cells (*arrow*) found in normal mouse brain (*; magnification, ×100). At high magnification (×400), hematoxylin-phloxin-saffron staining shows (*2*) that tumor is highly cellular with numerous mitoses, and presents an aggressive pattern (*3*) with limited area of necrosis (magnification, ×200). Some tumoral cells (*4*) had a membranous expression of CD133 (*arrows*). **B.** Immunoblotting was used to assess CD133 protein expression in lysates (20 μg proteins) generated from subcutaneous and intracerebral U87 glioblastoma-implanted or DAOY medulloblastoma-implanted cells as described in Materials and Methods. **C.** Lysates (5 μg protein) from *in vitro* cultured DAOY cell monolayers (*DAOY*), contralateral healthy brain (*Ctrl*), and from intracerebrally implanted DAOY cells (*Tumor*) were assessed for CD133 expression. Glyceraldehyde-3-phosphate dehydrogenase (*GAPDH*) expression was used as an internal loading control. **D.** Relative gene expression levels of CD133 (*CD133*), vascular endothelial growth factor (*VEGF*), and basic fibroblast growth factor (*bFGF*) were assessed by quantitative PCR using total RNA extracted from contralateral healthy brain (*white columns*) or from intracerebrally implanted DAOY tumors (*black columns*).

Glyceraldehyde-3-phosphate dehydrogenase protein expression was used as an internal loading control and remained unaffected throughout the conditions. When neurosphere-like formation was monitored, we found a significant decrease in neurosphere-like formation in cells whose MT1-MMP or MMP-9 had been silenced, as can be seen in images recorded at two different magnifications (×10 versus ×4; Fig. 3C). Cell migration was also assessed with mock-transfected cells as well as with DAOY monolayers and neurosphere-like DAOY cells that were transfected with MT1-MMP and MMP-9 silencers (Fig. 3D). The induced migration observed in neurosphere-like DAOY cells was completely abolished in those cells when either MT1-

MMP or MMP-9 gene expression was silenced (Fig. 3D, *neurospheres*). No significant decreases were observed in siMT1-MMP or in siMMP-9 DAOY cells from monolayer cultures (Fig. 3D, *monolayers*).

Overexpression of MT1-MMP Triggers Neurosphere-Like DAOY Differentiation

We further assessed the specific contribution of MT1-MMP toward the control of neurosphere-like DAOY formation. We first transiently transfected DAOY monolayers with cDNA encoding a recombinant MT1-MMP protein fused to green

fluorescent protein (GFP; ref. 23). Transfection efficiency was monitored using fluorescence microscopy and was confirmed by the expression of fluorescent cells (Fig. 4A). Moreover, recombinant MT1-MMP was also found to be active as its expression led to proMMP-2 activation and to an increase in proMMP-9 secretion as assessed by gelatin zymography (Fig. 4B). Mock- and MT1-MMP–transfected DAOY monolayers were then trypsinized and cultured either in monolayer medium or in neurosphere medium for 24 hours. Phase contrast pictures were taken in order to monitor for neurosphere-like formation in each culture condition. We found that mock-transfected cells were, as expected, still able to adhere and grow as monolayers when cultured in monolayer medium, although they formed neurosphere-like cells when cultured under neurosphere medium (Fig. 4C, *phase contrast pictures*). In contrast, when MT1-MMP–transfected DAOY monolayer cells were seeded in monolayer medium, we observed that very few GFP-positive cells adhered to the culture dishes but rather formed neurosphere-like cells (Fig. 4C, *phase contrast pictures*). This

was also evident through fluorescence visualization. Recombinant MT1-MMP overexpression was thus found to enhance neurosphere-like DAOY formation as shown through phase contrast and fluorescent microscopy imaging (Fig. 4C).

Discussion

Among brain tumors in children, the highly metastatic medulloblastomas represent ~25% of all pediatric intracranial neoplasms (24). Although modern neurosurgical and radiotherapy techniques combined with chemotherapy regimens result in prolonged free survival rates, the long-term prognosis is poor and the quality of life of these patients is generally poor (25). Recently, an isolated CD133(+) cell subpopulation from human brain tumors was shown to exhibit stem cell properties (5) and is thought to play a pivotal role in brain tumor initiation, growth, and recurrence (5, 26). Consequently, a better understanding of the potential contribution of brain tumor–derived CSC will help develop new clinical approaches in order
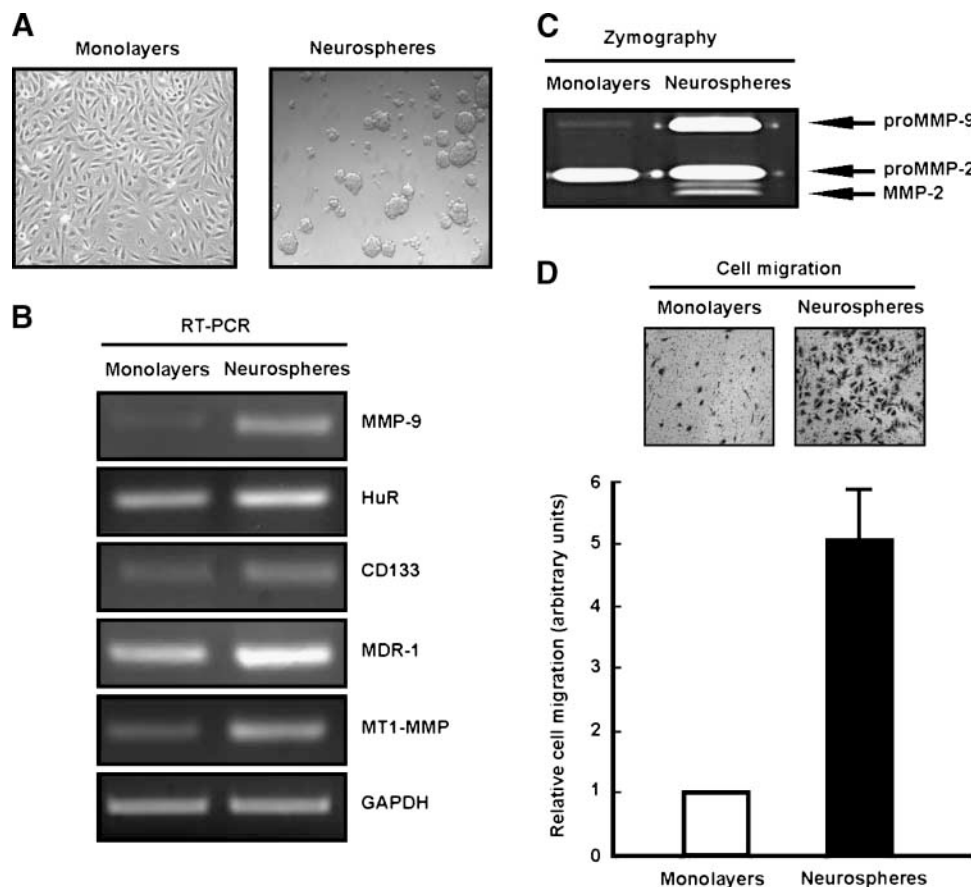

FIGURE 2. Increased CD133, MDR-1, MT1-MMP, and MMP-9 expression characterize the invasive phenotype of neurosphere-like DAOY cells. **A.** Representative phase contrast pictures of DAOY monolayers and neurosphere-like cells were taken after 48 h of culture. **B.** Total RNA was extracted from DAOY monolayers and neurosphere-like cells as described in Materials and Methods. Semiquantitative RT-PCR was done and cDNA amplicons for MMP-9, HuR, CD133, MDR-1, MT1-MMP, and glyceraldehyde-3-phosphate dehydrogenase were revealed by electrophoresis using agarose gels as described in Materials and Methods. **C.** Conditioned medium from DAOY monolayers and neurosphere-like cells were assessed for their MMP-9 and MMP-2 secretion and activation levels as described in Materials and Methods. **D.** DAOY monolayers and neurosphere-like cells were trypsinized and seeded (5 × 10⁴ cells) on gelatin-coated filters in modified Boyden chambers. Migration was allowed to proceed for 16 h at 37°C. Cells on filters were then fixed and stained; one out of five representative stainings for each condition. Columns, mean of a representative experiment in which five random fields per filter were counted for each condition; bars, SD.
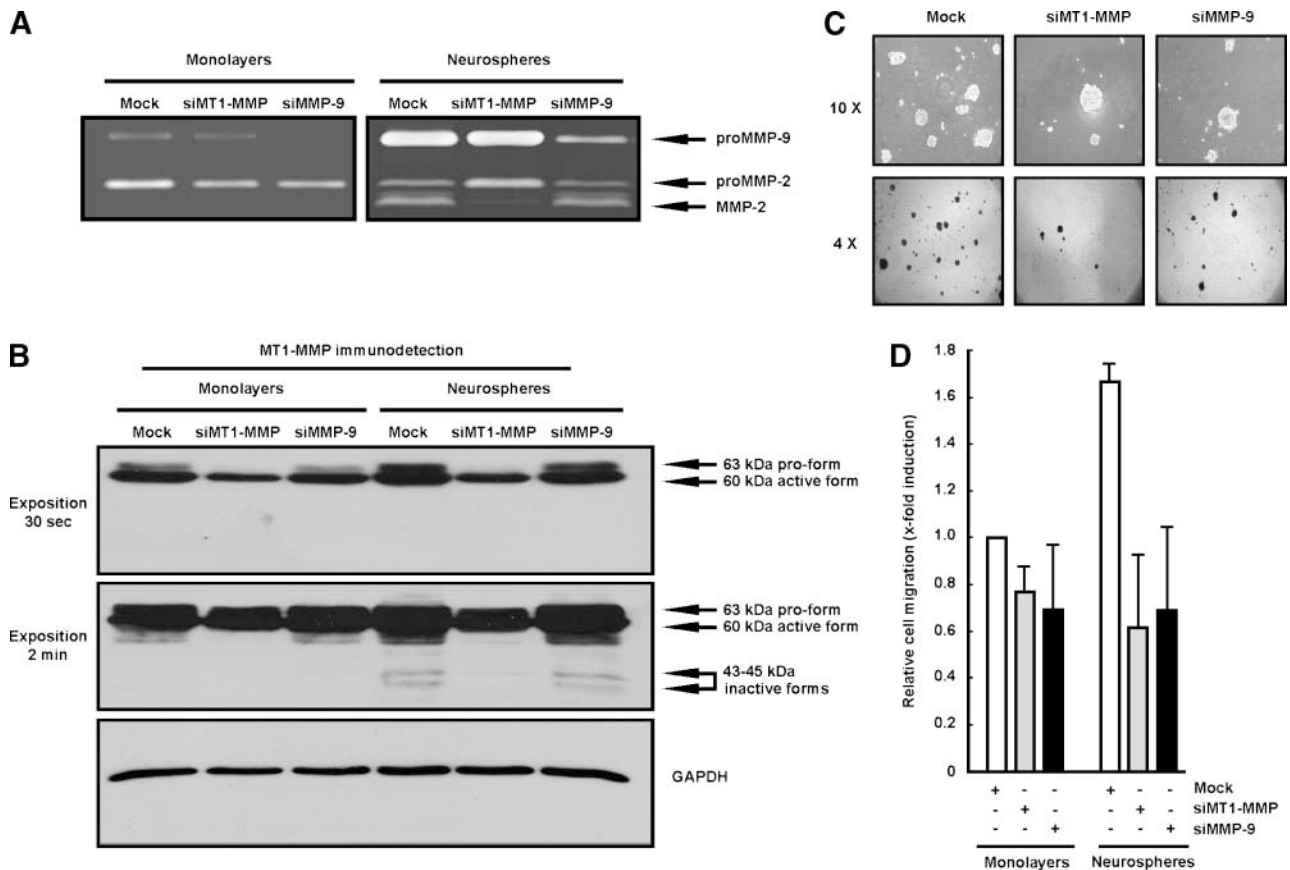
FIGURE 3. MT1-MMP and MMP-9 control the neurosphere-like formation process in DAOY cells and contribute to their invasive phenotype. **A.** Gene silencing using siRNA was used to down-regulate the expression of MT1-MMP and MMP-9 in DAOY cell monolayers (*top*) or DAOY neurospheres (*bottom*) as described in Materials and Methods. Conditioned medium from each respective condition was harvested 48 h posttransfection and the extent of either MT1-MMP or MMP-9 silencing assessed using gelatin zymography. **B.** MT1-MMP immunoblotting was done with cell lysates isolated from **A.** Autoradiograms are shown at 30-s vs. 2-min expositions in order to appreciate MT1-MMP down-regulation (30 s exposition), and the appearance of the 43 to 45 kDa inactive immunoreactive MT1-MMP that is generated during proMMP-2 activation (2 min exposition). Glyceraldehyde-3-phosphate dehydrogenase (GAPDH) was used as an internal loading control. **C.** Phase contrast (magnification, ×10 and ×4) microscopy enabled the visualization of the decrease in neurosphere-like formation in cells from which MT1-MMP or MMP-9 had been silenced. **D.** Cell migration was also assessed 48 h posttransfection in modified Boyden chambers as described in Materials and Methods for control (*white columns*) monolayers and neurosphere-like DAOY cells, and cells in which MMP-9 (*black columns*) and MT1-MMP (*gray columns*) gene expression was silenced. Columns, mean of a representative experiment in which five random fields per filter were counted for each condition; bars, SD.

to improve the efficiency of current treatment. In the present study, we identified and evaluated new biological and molecular features regulating the invasive phenotype associated with the formation of neurosphere-like CD133(+) medulloblastoma-derived CSC. Using RNA interference technology, we provided evidence for crucial roles for MMP-9 and for MT1-MMP, two major actors in cell invasion, metastasis, and resistance to radiation, in CD133(+) neurosphere-like formation in DAOY medulloblastoma cells.

It is noteworthy that as few as 100 CD133(+) cells from a brain tumor fraction were found to be capable of tumor initiation in nonobese diabetic/severe combined immunodeficiency mouse brains (5). The use of an intracerebral implantation model versus a flank implantation model in our current study, further added to the stringency of our experiments, proving that CD133 expression only arose from implanted brain tumor cells within a cerebral environment, possibly attributable to increased angiogenesis as reflected by

high vascular endothelial growth factor and basic fibroblast growth factor transcript levels. Gene expression profiles of experimental brain tumors grown as subcutaneous flank xenografts, intracerebral xenografts, and cells grown *in vitro* have been shown to be different suggesting that the tissue environment dictates the experimental tumor phenotype (27, 28). Intracerebral models can more closely mimic the actual environment of glioma- and medulloblastoma-derived CD133(+) CSC growth (29). The demonstration that CD133(+) cells express increased MDR-1 transcript levels (this study; ref. 30) also reveals issues important to drug delivery and to the blood-brain barrier environment that can now be addressed in terms of chemoresistance or angiogenic phenotype.

The CD133(+) fraction among medulloblastomas, which initiated tumors upon intracranial transplantation into the nonobese diabetic/severe combined immunodeficiency mouse forebrain, also correlated closely with an *in vitro* primary

sphere formation assay that was used to quantify stem cell properties (6). Although brain tumor stem cell properties have recently been studied in nonadherent neurospheres (31), the expression of selected markers was found to vary between nonadherent spheres and adherent monolayer cells, but no data was available as to MMP involvement in neurosphere-like formation. The identification and demonstration, in our current study, that MT1-MMP plays a role in medulloblastoma neurosphere-like formation provides support for the need to design new routes that use MT1-MMP as a therapeutic target. Indeed, based on blocking its activity with inhibitors, antibodies, or RNA interference, novel anticancer approaches using the inhibition of MT1-MMP activity have already been described (32). Work with MT1-MMP shows that interference with its RNA expression decreases tumor cell migration and invasion (33, 34). This approach has already been shown to be possible in endothelial cells in which interference of MT1-MMP RNA expression decreased the capacity to form capillary tubes in the Matrigel system (35). Although speculative, it is tempting to suggest that therapeutic use of interference RNA approaches could also target the MT1-MMP functions involved in the formation of neurosphere-like CD133(+) brain CSC.

Evidence provided from our own study suggests that inhibiting MT1-MMP and MMP-9 gene expression significantly impairs neurosphere-like formation and abrogates invasive properties (Fig. 3). The potential therapeutic use of interference RNA is currently being investigated (36-38).

It is still unclear whether CD133 expression plays a causative, contributing, or correlative role in the formation of the CSC population. Still, CD133-expressing CSC have been implicated in a number of key processes, including tumor repopulation, resistance to therapy, increased aggressiveness, and angiogenesis (5, 13). Among the important implications that arise from our study is the radioresistant phenotype ascribed to CD133-expressing CSC. A recent study has, in fact, provided evidence that CD133-expressing glioma cells *in vivo* and in culture are relatively resistant to radiation (13). Moreover, DAOY medulloblastoma cells that express CD133 were also shown to be radioresistant when compared with CD133(−) cells (4). Given that MT1-MMP expression is also correlated with brain tumor recurrence, increased invasiveness, and radioresistance (15), one can hypothesize in light of our observations that MT1-MMP triggers CD133(+) neurosphere-like formation in medulloblastoma cells, and that targeting of
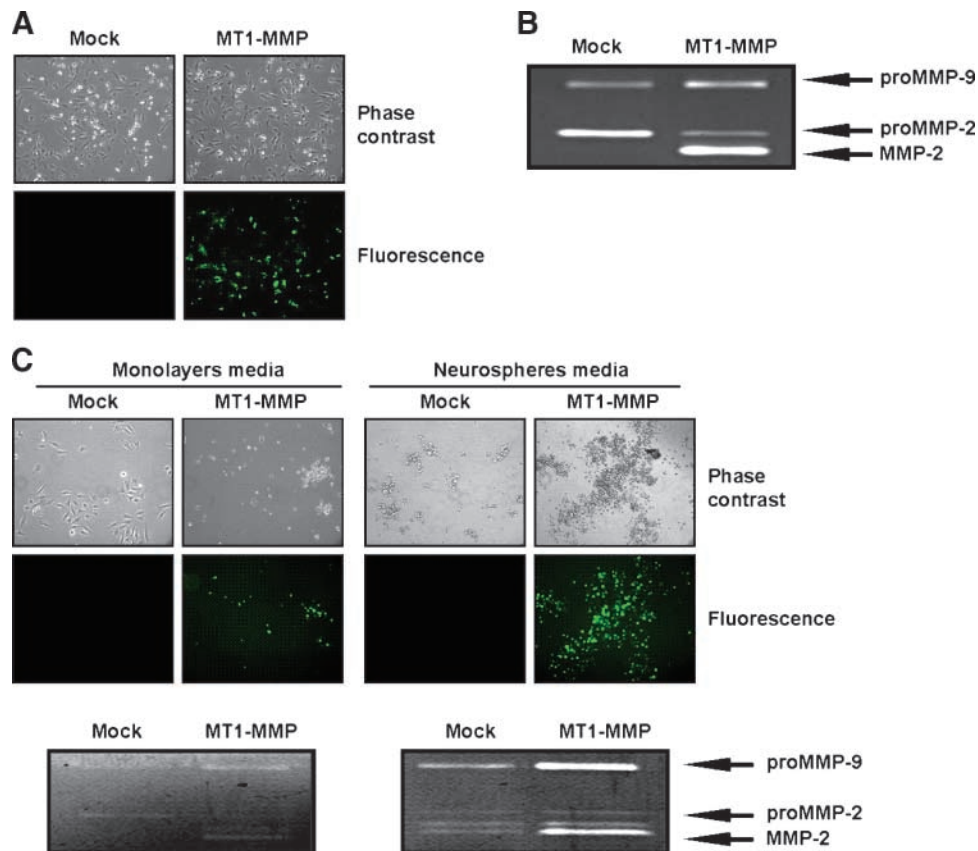

FIGURE 4. Overexpression of MT1-MMP triggers neurosphere-like DAOY differentiation. **A.** DAOY cell monolayers were transiently transfected with a plasmid encoding GFP-MT1-MMP as described in Materials and Methods. Representative pictures were taken in phase contrast (*top*) and fluorescence (*bottom*) in order to show transfection efficacy. **B.** Conditioned medium from mock and GFP-MT1-MMP−transfected cells were assessed for proMMP-2 activation by the expression of the recombinant MT1-MMP protein using gelatin zymography as described in Materials and Methods. **C.** Mock or GFP-MT1-MMP−transfected cells were trypsinized and then seeded either in monolayer medium or neurosphere medium. Representative pictures were then taken in phase contrast and fluorescence in order to monitor the extent of MT1-MMP−mediated neurosphere-like formation.

MT1-MMP functions and/or expression may alter the radio-resistant and invasive phenotype of brain CSC. As such, the expression of a major group of MT-MMP has recently been found elevated in gliomas (39), from which CD133(+) CSC isolated from fresh brain tumor specimens were found to escape the lethal damage of ionizing radiation (13). New possibilities for abrogating the tumor-promoting function of MT1-MMP, other than the conventional protease inhibitor-based approach, have recently been envisioned (32, 40, 41).

We have also identified increased levels of MMP-9 that correlated with neurosphere-like formation and to MT1-MMP increased expression. Known functions for MMP-9 include liberation of vascular endothelial growth factor during angiogenesis (42), and disruption of the blood-brain barrier (43, 44). More interesting are the less documented functions of MMP-9 recently reported in the promotion of thrombosis through increased tissue factor expression (45), the latter being thought to contribute to tumor growth/regulating properties of CD133(+) CSC through increased tissue factor–dependent procoagulant activity (46). In fact, clinical and experimental evidence suggests that high levels of tissue factor are correlated with increasing cancer aggressiveness and procoagulant tendencies (47). Furthermore, a crucial role of nuclear factor κB in tumor stem cell biology has recently been inferred in which it regulates the expression of genes that are involved in essential processes during the initiation and progression of various cancer types such as proliferation, migration, and apoptosis (48). Consistent with that observation, a correlation was found between proMMP-9 expression and MT1-MMP–mediated activation of proMMP-2 in specific conditions such as in 12-O-tetradecanoylphorbol-13-acetate–activated HT1080 fibrosarcoma cells (49). This phenomenon is thought to be mediated through nuclear factor κB activation (50, 51), and the promoter region of the MT1-MMP contains nuclear factor κB binding sites (52).

Finally, our study focused on the well-established method of neurosphere cell cultures that enabled us to study the *in vitro* CSC phenotype. As such, the successful isolation and establishment of a novel, long-term, primary, neurosphere-like cell line from highly aggressive anaplastic medulloblastoma was reported (53), and such a model will help shed light into the MMP functions of CD133(+) CSC. Our study is thus among the first to provide an *in vitro* model for potential MMP involvement in the CSC invasive phenotype. Direct evidence for the role of these MMPs will be obtained through the direct isolation and characterization of CD133(+) CSC. In conclusion, the involvement of MMP-9 and MT1-MMP in CD133(+) neurosphere formation and in their acquisition of an invasive phenotype and/or resistance to therapy phenotype could thus affect a provisional stem cell niche formation process that would, in part, support the emerging tumor. MMP-9 and MT1-MMP targeting in CSC may constitute promising new targets for anticancer therapies in destroying brain tumor stem cells.

Materials and Methods
Materials
SDS and bovine serum albumin were purchased from Sigma. Cell culture media was obtained from Life Technolo-gies. Electrophoresis reagents were purchased from Bio-Rad. The enhanced chemiluminescence reagents were from Amersham Pharmacia Biotech. Microbicinchoninic acid protein assay reagents were from Pierce. The polyclonal antibody against CD133 and the monoclonal antibody against glyceraldehyde-3-phosphate dehydrogenase were purchased from Abcam and Advanced Immunochemical, Inc., respectively. The polyclonal antibody against MT1-MMP (AB815) was from Chemicon. Horseradish peroxidase–conjugated donkey anti-rabbit and anti-mouse IgG secondary antibodies were from Jackson ImmunoResearch Laboratories. All other reagents were from Sigma-Aldrich, Canada.

Cell Culture and Neurosphere-Like Formation
The human DAOY medulloblastoma cell line was purchased from American Type Culture Collection and was maintained in Eagle's MEM containing 10% (v/v) calf serum (HyClone Laboratories), 2 mmol/L of glutamine, 100 units/mL of penicillin, and 100 mg/mL of streptomycin. Cells were incubated at 37°C, with 95% air and 5% CO_2. Neurosphere-like formation was triggered in a defined serum-free neural stem cell medium (54) containing Ex Vivo 15 (Lonza), 20 ng/mL of basic fibroblast growth factor, 20 ng/mL of epidermal growth factor (Wisent), 20 ng/mL of leukemia-inhibitory factor (Sigma), and 1× neural survival factor-1 (Lonza).

Intracranial Tumor Model
All animal experiments were evaluated and approved by the Institutional Committee for Good Animal Practices (Université du Québec à Montréal, Quebec, Canada). Intracerebral tumor implantation was done as previously described with some modifications (55). Anesthetized 5- to 10-week-old Crl:CD-1-nuBR female nude mice (Charles River) were placed in a stereotaxic frame; viable DAOY medulloblastoma (2×10^6) or U87 glioblastoma cells (5×10^4) in 5 μL of medium without serum were then implanted into the right corpus striatum at a depth of 3.5 mm at a point 2.5 mm lateral to the midline and 1.5 mm anterior to the bregma.

Subcutaneous Xenograft Model
Tumor implantation was done as described previously (56). Briefly, DAOY medulloblastoma or U87 glioblastoma cells were harvested by trypsinization using a trypsin/EDTA solution. Cells were washed thrice with PBS that was free of both Ca^{2+} and Mg^{2+}, and then centrifuged. The resulting pellet was resuspended in 1% methylcellulose in serum-free MEM at a concentration of 2.5×10^6 cells per 100 μL. Animals were anesthetized by oxygen/isoflurane inhalation and tumors were established by s.c. injection of 100 μL from the cell suspension into the right flank of female Crl:CD-1-nuBR nude mice.

Histology and Immunocytochemistry
Mouse brains were fixed in 10% buffered formalin and paraffin-embedded. For routine histologic examination, 3-μm-thick sections were stained with hematoxylin-phloxin-saffron. Immunohistochemistry was done on paraffin-embedded sections using the biotin-streptavidin peroxidase LSAB kit in conjunction with an automated DAKO immunostainer

(DakoCytomation). An antibody against CD133 (1:100, rabbit polyclonal; Abcam) was applied. First, for antigen retrieval, deparaffinized and rehydrated sections were treated using a pressure cooker [citrate buffer (pH 6.0), 1:10, 30 min]. Then the sections were mounted in the DAKO autostainer, covered with H_2O_2 for 5 min, followed by a 5-min application of Ultra V block (LabVision). The slides were then incubated for 60 min with the diluted antibody at room temperature, followed by application of the labeled biotin-streptavidin reagents according to the manufacturer's instructions (LSAB+ System HRP-Kit; DAKO). 3,3′-Diaminobenzidine (DAKO) was used as a chromogen. A section of human fetal liver was used in the same slide as a specific, positive control (57). Normal mouse or rabbit IgG at the same concentration as the primary antibody served as negative controls. Slides were then incubated with this solution instead of primary antibody. Tissues were analyzed and photographed using a Zeiss Axioplan microscope.

Total RNA Isolation and Semiquantitative RT-PCR Analysis

Total RNA was extracted from monolayers or neurosphere-like DAOY cells using the TRIzol reagent (Life Technologies). One microgram of total RNA was used for first-strand cDNA synthesis followed by specific gene product amplification with the One-step RT-PCR Kit (Invitrogen). Primers for CD133 (Santa Cruz Biotechnology), MDR-1 (forward, 5′-ATTCAAC-TATCCCACCCGACCG-3′; reverse, 5′-CCTTTGCTGCCC-TCACAATCTC-3′), MT1-MMP (forward, 5′-ATTGATGCT-GCTCTCTTCTGG-3′; reverse, 5′-GTGAAGACTTCATCG-CTGCC-3′), HuR (forward, 5′-TCGCAGCTGTACCACTCGC-CAG-3′; reverse, 5′-CCAAACATCTGCCAGAGGATC-3′), and for MMP-9 (forward, 5′-AAGATGCTGCTGTTCAGC-GGG-3′; reverse, 5′-GTCCTCAGGGCACTGCAGGAT-3′) were all derived from human sequences. PCR conditions were optimized so that the gene products were examined at the exponential phase of their amplification and the products were resolved on 1.8% agarose gels containing 1 μg/mL of ethidium bromide.

cDNA Synthesis and Real-time Quantitative RT-PCR

Total RNA was extracted from fresh tumor tissue or cell cultures as described above. For cDNA synthesis, ~ 1 μg total RNA was reverse-transcribed into cDNA using high-capacity cDNA reverse transcription kit (Applied Biosystems). cDNA was stored at −80°C for PCR. Gene expression was quantified by real-time quantitative PCR using iQ SYBR Green Supermix (Bio-Rad). DNA amplification was carried out using Icycler iQ5 (Bio-Rad) and product detection was done by measuring the binding of the fluorescent dye SYBR Green I to double-stranded DNA. All the primer sets were provided by Qiagen. The relative quantities of target gene mRNA against an internal control, 18S rRNA, were measured by following a ΔC_T method. An amplification plot that had been the plot of fluorescence signal versus cycle number was drawn. The difference (ΔC_T) between the mean values in the triplicate samples of target gene and those of 18S rRNA were calculated by iQ5 Optical System Software version 2.0 (Bio-Rad) and the relative quantified value was expressed as $2^{\Delta C_T}$.

RNA Interference

RNA interference experiments were done using HiPerFect (Qiagen). A small interfering RNA (20 nmol/L) against MT1-MMP (siMT1-MMP) and mismatch small interfering RNA were synthesized by EZBiolab Inc., and annealed to form duplexes. The sequence of the siMT1-MMP used in this study was derived from the human MT1-MMP gene (NM_004995) and is as follows: 5′-CCAGAAGCUGAAGGUAGAAdTdT-3′ (sense) and 5′-UUCUACCUUCAGCUUCUGGdTdT-3′ (anti-sense; ref. 58). A small interfering RNA against human MMP-9 (siMMP-9; GenBank accession number, NM-004994) and mismatch small interfering RNA with no known homology to mammalian genes were synthesized (Qiagen) against the following published target sequences for MMP-9: 5′-AACAT-CACCTATTGGATCCAAACTAC-3′, nucleotides 377 to 403. The sequence of the siMMP-9 used in this study is as follows: 5′-CAUCACCUAUUGGAUCCAAdTdT-3′ (sense) and 5′-UUGGAUCCAAUAGGUGAUGdTdT-3′ (antisense). Evaluation of the transient knockdown duration was done by real-time quantitative RT-PCR, and the targeted gene expression was found to be routinely diminished by 65% to 90%, 24 to 48 h posttransfection (data not shown).

Cell Transfection Method

Subconfluent DAOY monolayer cells were transiently transfected with 10 μg of the cDNA encoding the full-length (Wt) MT1-MMP fused to GFP (59) using LipofectAMINE 2000 (Invitrogen). Mock transfections of U87 cultures with pcDNA (3.1+) were used as controls. Transfected cells were left to recuperate and were used 48 h posttransfection. The occurrence of MT1-MMP–specific gene expression and function was evaluated by semiquantitative RT-PCR, immunoblotting procedures, and validated by assessing MT1-MMP–mediated proMMP-2 activation by gelatin zymography (Figs. 3 and 4).

Gelatin Zymography

Gelatin zymography was used to assess the proMMP-9, proMMP-2, and MMP-2 extracellular levels. Briefly, an aliquot (20 μL) of the culture medium was subjected to SDS-PAGE in a gel containing 0.1 mg/mL of gelatin. The gels were then incubated in 2.5% Triton X-100 and rinsed in nanopure distilled H_2O. Gels were further incubated at 37°C for 20 h in 20 mmol/L of NaCl, 5 mmol/L of $CaCl_2$, 0.02% Brij-35, 50 mmol/L of Tris-HCl buffer (pH 7.6), then stained with 0.1% Coomassie brilliant blue R-250, and destained in 10% acetic acid and 30% methanol in H_2O. Gelatinolytic activity was detected as unstained bands on a blue background.

Immunoblotting Procedures

Proteins from control and treated cells were separated by SDS-PAGE. After electrophoresis, proteins were electrotransferred to polyvinylidene difluoride membranes which were then blocked for 1 h at room temperature with 5% nonfat dry milk in TBS (150 mmol/L NaCl, 20 mmol/L Tris-HCl; pH 7.5) containing 0.3% Tween 20 (TBST). Membranes were further washed in TBST and incubated with the primary antibodies (1:1,000 dilution) in TBST containing 3% bovine serum albumin, followed by a 1-h incubation with horseradish

peroxidase–conjugated antirabbit or antimouse IgG (1:2,500 dilution) in TBST containing 5% nonfat dry milk. Immunoreactive material was visualized by enhanced chemiluminescence (Amersham Biosciences).

Analysis of DAOY Cell Migration

DAOY cell migration was assessed using modified Boyden chambers. The lower surfaces of transwells (8-μm pore size; Costar) were precoated with 1 mg/mL of gelatin for 2 h at 37°C. The transwells were then assembled in a 24-well plate (Fisher Scientific, Ltd.). The lower chamber was filled with serum-free medium. Monolayer or neurosphere-like DAOY cells were collected by trypsinization, washed, and resuspended in serum-free medium at a concentration of 5×10^5 cells/mL; 5×10^4 cells were then inoculated onto the upper side of each modified Boyden chamber. The plates were placed at 37°C in 5% CO_2/95% air and migration left to proceed for 16 h. Cells that had migrated to the lower surfaces of the filters were fixed with 10% formalin phosphate and stained with 0.1% crystal violet-20% methanol (v/v). Images of at least five random fields per filter were digitized (100× magnification). The average number of migrating cells per field was quantified using Northern Eclipse software (Empix Imaging Inc.). Migration data are expressed as a mean value derived from at least three independent experiments.

Statistical Data Analysis

Data are representative of three or more independent experiments. Statistical significance was assessed using Student's unpaired *t* test. Probability values of <0.05 were considered significant, and an asterisk (*) identifies such significance in each figure.

Disclosure of Potential Conflicts of Interest
No potential conflicts of interest were disclosed.

Acknowledgments

References
1. Hemmati HD, Nakano I, Lazareff JA, et al. Cancerous stem cells can arise from pediatric brain tumors. Proc Natl Acad Sci U S A 2003;100:15178–83.

2. Yuan X, Curtin J, Xiong Y, et al. Isolation of cancer stem cells from adult glioblastoma multiforme. Oncogene 2004;23:9392–400.

3. Dean M, Fojo T, Bates S. Tumour stem cells and drug resistance. Nat Rev Cancer 2005;5:275–84.

4. Blazek ER, Foutch JL, Maki G. Daoy medulloblastoma cells that express CD133 are radioresistant relative to CD133− cells, and the CD133+ sector is enlarged by hypoxia. Int J Radiat Oncol Biol Phys 2007;67:1–5.

5. Singh SK, Hawkins C, Clarke ID, et al. Identification of human brain tumour initiating cells. Nature 2004;432:396–401.

6. Singh S, Dirks PB. Brain tumor stem cells: identification and concepts. Neurosurg Clin N Am 2007;18:31–8.

7. Nakada M, Okada Y, Yamashita J. The role of matrix metalloproteinases in glioma invasion. Front Biosci 2003;8:e261–9.

8. Lakka SS, Gondi CS, Rao JS. Proteases and glioma angiogenesis. Brain Pathol 2005;15:327–41.

9. Bodey B, Bodey B, Jr., Siegel SE, Kaiser HE. Matrix metalloproteinase expression in childhood medulloblastomas/primitive neuroectodermal tumors. In Vivo 2000;14:667–73.

10. Vince GH, Herbold C, Klein R, et al. Medulloblastoma displays distinct regional matrix metalloprotease expression. J Neurooncol 2001;53:99–106.

11. Ozen O, Krebs B, Hemmerlein B, Pekrun A, Kretzschmar H, Herms J. Expression of matrix metalloproteinases and their inhibitors in medulloblastomas and their prognostic relevance. Clin Cancer Res 2004;10:4746–53.

12. Rao JS, Bhoopathi P, Chetty C, Gujrati M, Lakka SS. MMP-9 short interfering RNA induced senescence resulting in inhibition of medulloblastoma growth via p16(INK4a) and mitogen-activated protein kinase pathway. Cancer Res 2007;67:4956–64.

13. Bao S, Wu Q, McLendon RE, et al. Glioma stem cells promote radioresistance by preferential activation of the DNA damage response. Nature 2006;444:756–60.

14. Wild-Bode C, Weller M, Rimner A, Dichgans J, Wick W. Sublethal irradiation promotes migration and invasiveness of glioma cells: implications for radiotherapy of human glioblastoma. Cancer Res 2001;61:2744–50.

15. Annabi B, Lee YT, Martel C, Pilorget A, Bahary JP, Beliveau R. Radiation induced-tubulogenesis in endothelial cells is antagonized by the antiangiogenic properties of green tea polyphenol (−) epigallocatechin-3-gallate. Cancer Biol Ther 2003;2:642–9.

16. Annabi B, Thibeault S, Moumdjian R, Beliveau R. Hyaluronan cell surface binding is induced by type I collagen and regulated by caveolae in glioma cells. J Biol Chem 2004;279:21888–96.

17. Annabi B, Bouzeghrane M, Moumdjian R, Moghrabi A, Beliveau R. Probing the infiltrating character of brain tumors: inhibition of RhoA/ROK-mediated CD44 cell surface shedding from glioma cells by the green tea catechin EGCg. J Neurochem 2005;94:906–16.

18. Annabi B, Lachambre MP, Bousquet-Gagnon N, Page M, Gingras D, Beliveau R. Green tea polyphenol (−)-epigallocatechin 3-gallate inhibits MMP-2 secretion and MT1-MMP-driven migration in glioblastoma cells. Biochim Biophys Acta 2002;1542:209–20.

19. Annabi B, Currie JC, Moghrabi A, Beliveau R. Inhibition of HuR and MMP-9 expression in macrophage-differentiated HL-60 myeloid leukemia cells by green tea polyphenol EGCg. Leuk Res 2007;31:1285–92.

20. Milosevic J, Storch A, Schwarz J. Spontaneous apoptosis in murine free-floating neurospheres. Exp Cell Res 2004;294:9–17.

21. Beier D, Hau P, Proescholdt M, et al. CD133(+) and CD133(−) glioblastoma-derived cancer stem cells show differential growth characteristics and molecular profiles. Cancer Res 2007;67:4010–5.

22. Gal H, Makovitzki A, Amariglio N, Rechavi G, Ram Z, Givol D. A rapid assay for drug sensitivity of glioblastoma stem cells. Biochem Biophys Res Commun 2007;358:908–13.

23. Belkaid A, Fortier S, Cao J, Annabi B. Necrosis induction in glioblastoma cells reveals a new "bioswitch" function for the MT1-MMP/G6PT signaling axis in proMMP-2 activation versus cell death decision. Neoplasia 2007;9: 332–40.

24. Saran F. Recent advances in paediatric neuro-oncology. Curr Opin Neurol 2002;15:671–7.

25. Kuhl J, Doz F, Taylor RE. Embryonic tumors. In: Walker D, Perilongo G, Punt JAG, Taylor GE, editors. Brain and spinal tumors of childhood. Arnold, London: 2004. p. 314–30.

26. Liu G, Yuan X, Zeng Z, et al. Analysis of gene expression and chemoresistance of CD133+ cancer stem cells in glioblastoma. Mol Cancer 2006;5:67.

27. Ozawa T, Wang J, Hu LJ, Lamborn KR, Bollen AW, Deen DF. Characterization of human glioblastoma xenograft growth in athymic mice. In Vivo 1998;12:369–74.

28. Camphausen K, Purow B, Sproull M, et al. Influence of *in vivo* growth on human glioma cell line gene expression: convergent profiles under orthotopic conditions. Proc Natl Acad Sci U S A 2005;102:8287–92.

29. Koutcher JA, Hu X, Xu S, et al. MRI of mouse models for gliomas shows similarities to humans and can be used to identify mice for preclinical trials. Neoplasia 2002;4:480–5.

30. Salmaggi A, Boiardi A, Gelati M, et al. Glioblastoma-derived tumorospheres identify a population of tumor stem-like cells with angiogenic potential and enhanced multidrug resistance phenotype. Glia 2006;54:850–60.

31. Inagaki A, Soeda A, Oka N, et al. Long-term maintenance of brain tumor stem cell properties under at non-adherent and adherent culture conditions. Biochem Biophys Res Commun 2007;361:586–92.

32. Arroyo AG, Genis L, Gonzalo P, Matias-Roman S, Pollan A, Galvez BG. Matrix metalloproteinases: new routes to the use of MT1-MMP as a therapeutic target in angiogenesis-related disease. Curr Pharm Des 2007;13:1787–802.

33. Ueda J, Kajita M, Suenaga N, Fujii K, Seiki M. Sequence-specific silencing

of MT1-MMP expression suppresses tumor cell migration and invasion: importance of MT1-MMP as a therapeutic target for invasive tumors. Oncogene 2003;22:8716 – 22.

34. Bartolome RA, Molina-Ortiz I, Samaniego R, Sanchez-Mateos P, Bustelo XR, Teixido J. Activation of Vav/Rho GTPase signaling by CXCL12 controls membrane-type matrix metalloproteinase-dependent melanoma cell invasion. Cancer Res 2006;66:248 – 58.

35. Robinet A, Fahem A, Cauchard JH, et al. Elastin-derived peptides enhance angiogenesis by promoting endothelial cell migration and tubulogenesis through upregulation of MT1-MMP. J Cell Sci 2005;118:343 – 56.

36. Uprichard SL. The therapeutic potential of RNA interference. FEBS Lett 2005;579:5996 – 6007.

37. Lu PY, Xie FY, Woodle MC. Modulation of angiogenesis with siRNA inhibitors for novel therapeutics. Trends Mol Med 2005;11:104 – 13.

38. Lu PY, Xie F, Woodle MC. *In vivo* application of RNA interference: from functional genomics to therapeutics. Adv Genet 2005;54:117 – 42.

39. Nuttall RK, Pennington CJ, Taplin J, et al. Elevated membrane-type matrix metalloproteinases in gliomas revealed by profiling proteases and inhibitors in human cancer cells. Mol Cancer Res 2003;1:333 – 45.

40. Nonaka T, Nishibashi K, Itoh Y, Yana I, Seiki M. Competitive disruption of the tumor-promoting function of membrane type 1 matrix metalloproteinase/matrix metalloproteinase-14 *in vivo*. Mol Cancer Ther 2005;4:1157 – 66.

41. Hatakeyama H, Akita H, Ishida E, et al. Tumor targeting of doxorubicin by anti-MT1-MMP antibody-modified PEG liposomes. Int J Pharm 2007;342:194 – 200.

42. Bergers G, Brekken R, McMahon G, et al. Matrix metalloproteinase-9 triggers the angiogenic switch during carcinogenesis. Nat Cell Biol 2000;2:737 – 44.

43. Valable S, Montaner J, Bellail A, et al. VEGF-induced BBB permeability is associated with an MMP-9 activity increase in cerebral ischemia: both effects decreased by Ang-1. J Cereb Blood Flow Metab 2005;25:1491 – 504.

44. Shigemori Y, Katayama Y, Mori T, Maeda T, Kawamata T. Matrix metalloproteinase-9 is associated with blood-brain barrier opening and brain edema formation after cortical contusion in rats. Acta Neurochir Suppl 2006;96:130 – 3.

45. Morishige K, Shimokawa H, Matsumoto Y, et al. Overexpression of matrix metalloproteinase-9 promotes intravascular thrombus formation in porcine coronary arteries *in vivo*. Cardiovasc Res 2003;57:572 – 85.

46. Milsom C, Anderson GM, Weitz JI, Rak J. Elevated tissue factor procoagulant activity in CD133-positive cancer cells. J Thromb Haemost 2007;5:2550 – 2.

47. Rak J, Milsom C, May L, Klement P, Yu J. Tissue factor in cancer and angiogenesis: the molecular link between genetic tumor progression, tumor neovascularization, and cancer coagulopathy. Semin Thromb Hemost 2006;32:54 – 70.

48. Dolcet X, Llobet D, Pallares J, Matias-Guiu X. NF-kB in development and progression of human cancer. Virchows Arch 2005;446:475 – 82.

49. Park BC, Thapa D, Lee YS, et al. 1-Furan-2-yl-3-pyridin-2-yl-propenone inhibits the invasion and migration of HT1080 human fibrosarcoma cells through the inhibition of proMMP-2 activation and down regulation of MMP-9 and MT1-MMP. Eur J Pharmacol 2007;567:193 – 7.

50. Lee KW, Kim JH, Lee HJ, Surh YJ. Curcumin inhibits phorbol ester-induced up-regulation of cyclooxygenase-2 and matrix metalloproteinase-9 by blocking ERK1/2 phosphorylation and NF-κB transcriptional activity in MCF10A human breast epithelial cells. Antioxid Redox Signal 2005;7:1612 – 20.

51. Park JM, Kim A, Oh JH, Chung AS. Methylseleninic acid inhibits PMA-stimulated pro-MMP-2 activation mediated by MT1-MMP expression and further tumor invasion through suppression of NF-κB activation. Carcinogenesis 2007;28:837 – 47.

52. Han YP, Tuan TL, Wu H, Hughes M, Garner WL. TNF-α stimulates activation of pro-MMP2 in human skin through NF-(κ)B mediated induction of MT1-MMP. J Cell Sci 2001;114:131 – 9.

53. Raso A, Negri F, Gregorio A, et al. Successful isolation and long-term establishment of a cell line with stem cell-like features from an anaplastic medulloblastoma. Neuropathol Appl Neurobiol 2008;34:306 – 15.

54. Rietze RL, Reynolds BA. Neural stem cell isolation and characterization. Methods Enzymol 2006;419:3 – 23.

55. Regina A, Demeule M, Berube A, Moumdjian R, Berthelet F, Beliveau R. Differences in multidrug resistance phenotype and matrix metalloproteinases activity between endothelial cells from normal brain and glioma. J Neurochem 2003;84:316 – 24.

56. Rolland Y, Demeule M, Michaud-Levesque J, Beliveau R. Inhibition of tumor growth by a truncated and soluble form of melanotransferrin. Exp Cell Res 2007;313:2910 – 9.

57. Shmelkov SV, Meeus S, Moussazadeh N, et al. Cytokine preconditioning promotes codifferentiation of human fetal liver CD133+ stem cells into angiomyogenic tissue. Circulation 2005;111:1175 – 83.

58. Neth P, Ciccarella M, Egea V, Hoelters J, Jochum M, Ries C. Wnt signaling regulates the invasion capacity of human mesenchymal stem cells. Stem Cells 2006;24:1892 – 903.

59. Cao J, Chiarelli C, Kozarekar P, Adler HL. Membrane type 1-matrix metalloproteinase promotes human prostate cancer invasion and metastasis. Thromb Haemost 2005;93:770 – 8.